Received: 1 February 2023 | Revised: 16 May 2023 | Accepted: 30 May 2023

DOI: 10.1002/biot.202300051

Biotechnology Journal

RESEARCH ARTICLE

Production of adeno-associated viral vector serotype 6 by triple transfection of suspension HEK293 cells at higher cell densities

Pablo D. Moço[1] | **Xingge Xu**[1] | **Cristina A. T. Silva**[1,2] | **Amine A. Kamen**[1]

[1]Department of Bioengineering, McGill University, Montreal, Canada

[2]Department of Chemical Engineering, Polytechnique Montréal, Montreal, Canada

Correspondence
Amine Kamen, Department of Bioengineering, McGill University, McConnell Engineering Building, Room 363, 3480 University Street, Montreal, QC H3A 0E9, Canada.
Email: amine.kamen@mcgill.ca

Funding information
Canada Research Chairs, Grant/Award Number: CRC-240394.; Natural Sciences and Engineering Research Council of Canada, Grant/Award Number: RGPIN-2021-02691

Abstract

In recent years, the use of adeno-associated viruses (AAVs) as vectors for gene and cell therapy has increased, leading to a rise in the amount of AAV vectors required during pre-clinical and clinical trials. AAV serotype 6 (AAV6) has been found to be efficient in transducing different cell types and has been successfully used in gene and cell therapy protocols. However, the number of vectors required to effectively deliver the transgene to one single cell has been estimated at 10^6 viral genomes (VG), making large-scale production of AAV6 necessary. Suspension cell-based platforms are currently limited to low cell density productions due to the widely reported cell density effect (CDE), which results in diminished production at high cell densities and decreased cell-specific productivity. This limitation hinders the potential of the suspension cell-based production process to increase yields. In this study, we investigated the improvement of the production of AAV6 at higher cell densities by transiently transfecting HEK293SF cells. The results showed that when the plasmid DNA was provided on a cell basis, the production could be carried out at medium cell density (MCD, 4×10^6 cells mL^{-1}) resulting in titers above 10^{10} VG mL^{-1}. No detrimental effects on cell-specific virus yield or cell-specific functional titer were observed at MCD production. Furthermore, while medium supplementation alleviated the CDE in terms of VG/cell at high cell density (HCD, 10×10^6 cells mL^{-1}) productions, the cell-specific functional titer was not maintained, and further studies are necessary to understand the observed limitations for AAV production in HCD processes. The MCD production method reported here lays the foundation for large-scale process operations, potentially solving the current vector shortage in AAV manufacturing.

KEYWORDS
adeno-associated virus, bioprocess development, cell density effect, suspension cells, transient transfection

ABBREVIATIONS: AAV, adeno-associated virus; AAV6, AAV serotype 6; CDE, cell density effect; CSVY, cell-specific virus yield; ETU, enhanced transducing units; FDA, US Food and Drug Administration; GFP, green fluorescent protein; GOI, gene of interest; HCD, high cell density; LCD, low cell density; MCD, medium cell density; PEI, polyethylenimine; VG, viral genomes.

1 | INTRODUCTION

Adeno-associated viruses (AAVs) are small, 25-nm-wide, icosahedral, non-enveloped viruses with a 4.7-kb-long single-stranded DNA genome, who belong to the family *Parvoviridae*.[1] AAVs are non-pathogenic and replication-defective,[2] depending on co-infection with helper viruses, such as adenovirus or herpes simplex virus. First discovered from stocks of adenovirus in the 1960s,[2,3] AAVs have recently become a critical gene delivery vector for treating diseases. Glybera was the first AAV-based gene therapy drug approved in 2012 by the European Medicines Agency.[4].The US Food and Drug Administration (FDA) approved 2 AAV-based gene therapy drugs, Luxturna, in 2017[5] and, Zolgesma, in 2019.[6]

To this date, based on phylogenetic analysis, 13 different serotypes and more than 100 variants of AAV have been identified.[2,3,7–14] Due to heterogeneity in capsid proteins, each serotype exhibits a distinct tropism and ability to transduce different cell types.[15] Serotype 6 has a wide range of target cells and has been shown to successfully transduce cells in the central nervous system,[16] human prostate, breast, and liver cancer cells,[17] melanocytes,[18] skeletal muscle,[19–21] heart,[22–24] lung,[25] and the eye.[26] Recently, AAV serotype 6 (AAV6) gained popularity due to its ability to transduce lymphocytes[27–29] and its use for generating Chimeric Antigen Receptor T cells.[30–36]

The number of therapeutic AAV applications being investigated is steadily increasing, with more than 300 completed or ongoing clinical trials.[37] These applications require large amounts of AAV vectors to validate pre-clinical animal studies and clinical trials. Reported doses can reach up to 7.5×10^{15} viral genomes (VG) for targeted delivery and up to 1.5×10^{17} VG for systemic delivery.[38] This large requirement in the number of viral vectors implies that an improvement in current production methods is necessary. This is especially true for AAV6, which requires up to 10^6 VG cell^{-1} during the transduction of T cells.[27] Recombinant AAV is produced by replacing the viral genes, *Rep* and *Cap*, with the gene of interest (GOI). Mammalian cells are transiently transfected with a GOI cassette flanked by the inverted terminal repeats, a plasmid carrying the *Rep* and *Cap* functions, and a third plasmid encoding the helper functions.[39–42] The transient transfection is generally done using the cost-effective cationic polymer, polyethylenimine (PEI).[43] However, adherent cell cultures are not deemed viable for AAV production at scales that exceed 10^{15} total VGs, making them unsuitable for late-phase clinical trials and commercial applications of these viral vectors.[44] The use of HEK293 cells in suspension for producing AAV vectors was first described in 2006.[45] Despite many efforts in optimizing production, large-scale production of AAV vectors is considered a bottleneck in their implementation as a widespread type of viral vector for gene therapy and cell therapy,[46] mainly because current HEK293-based production is done at low cell densities.[45,47–51] Limiting the production of viral vectors to lower cell densities hinders the potential of this production process to be intensified.[52] On the other hand, the production of viral vectors at higher cell densities tends to be limited by the widely reported cell density effect (CDE), which results in diminished transfection and productivity.[53–55] In this study, we demonstrate that the production of AAV6 via transient transfection of suspension HKE293SF cells is not limited to low cell density (LCD) cultures. No CDE is observed when cells are transfected at 4×10^6 cells mL^{-1} with 1 μg of plasmid DNA per 10^6 cells.

2 | MATERIAL AND METHODS

2.1 | Cell line and culture

HEK293SF-3F6 (HEK293SF) cells were kindly provided by the National Research Council Canada[56] and maintained in serum-free suspension cultures at 37°C, 5% CO_2, and 75% relative humidity in a shaker incubator (Infors, Switzerland) at 135 rpm speed of agitation or specified otherwise. Cells were maintained at exponential growth phase (between 0.25 and 2×10^6 cells mL^{-1}) by splitting every 4 days. Cells at a maximum passage of 15 (post-thawing) were used for transfection experiments. The basal maintenance and production medium was HyCell TransFx-H (Cytiva Life Sciences, USA) supplemented with 0.1% w/v of Kolliphor P188 (Sigma–Aldrich, USA) and 4 mM GlutaMAX (Gibco, USA). GlutaMAX was replaced by 6 mM L-glutamine (Gibco, USA) for experiments in which nutrients and metabolites were analyzed. The supplemented medium was prepared by adding either glucose for a final concentration of 7.2 g L^{-1} (40 mM) or 15% v/v Cell Boost 5 (Cytiva Life Sciences, USA) to achieve a similar glucose concentration.

Low (LCD) and medium cell density (MCD) cultures (1 and 4×10^6 cells mL^{-1}, respectively, at the time of transfection – TOT) were done in 125-mL polycarbonate shake flasks (TriForest, USA) with a working volume of 25 mL. For MCD, the cells were concentrated and inoculated at the desired concentration in fresh medium immediately before transfection to prevent any detrimental effects from spent medium. High cell density (HCD, 10×10^6 cells mL^{-1} at TOT) transfection was performed in 50-mL TubeSpin bioreactors (TPP, Switzerland) with a working volume of 10 mL and 180 rpm. For achieving and maintaining high cell densities, from 48 h post-seeding, a pseudo-perfusion was conducted with medium exchange of 1 vessel volume per day (VVD) both before and after transfection, where cells were centrifuged at $300 \times g$ for 5 min and resuspended in fresh medium.

The bioreactor production was performed in a 3-L vessel (Applikon Biotechnology, The Netherlands) equipped with a double marine impeller with 45-mm outer diameter, a pH sensor, a temperature sensor, a dissolved oxygen (DO) concentration sensor, a microsparger with 100-nm pore size, and a capacitance probe for monitoring of cell

culture characteristics, such as cell growth. The impeller speed was set between 100 and 120 rpm clockwise. The pH and temperature parameters were set at 7.15 ± 0.05 and 37°C, respectively. The overlay air flow was maintained at 12.5 mL min^{-1}. The oxygen flow into the sparger was controlled by a one-way PID control loop with DO set 40% oxygen saturation. The maximum oxygen flow was 100 mL min^{-1} when PID output was 100%. In order to accurately reproduce the small-scale experiments, the HEK293SF cells from shake flasks were inoculated into the bioreactor at 4×10^6 cells mL^{-1} in a fresh culture medium. The transfection was conducted immediately after cell inoculation with plasmid delivered on a cell basis (1 $\mu g/10^6$ cells).

2.2 | Plasmids

The following plasmids were used to produce adeno-associated viral vectors: (1) pAdDeltaF6 was a gift from James M. Wilson (Addgene plasmid #112867; http://n2t.net/addgene:112867; RRID:Addgene_112867), (2) pRep2Cap6 (provided by Dr. Samulski, University of North Carolina, USA), (3) pAAV-CAG-GFP was a gift from Edward Boyden (Addgene plasmid #37825; http://n2t.net/addgene:37825; RRID:Addgene_37825), and (4) pX601-AAV-saCas9-sgRNA, modified from pX601-AAV-CMV::NLS-SaCas9-NLS-3xHA-bGHpA;U6::BsaI-sgRNA, a gift from Feng Zhang (Addgene plasmid #61591; http://n2t.net/addgene:61591; RRID:Addgene_61591).

2.3 | Transient transfection

Recombinant AAV6 particles expressing green fluorescent protein (GFP) driven by the CAG promoter were produced via triple transient transfection of HEK293SF cells as previously described.[57] In brief, the transgene plasmid pAAV-CAG-GFP, the plasmid pRep2Cap6, and the helper plasmid pAdDeltaF6 were co-transfected into HEK293SF cells in a ratio of 1:1:1 after complexation with 25-kDa linear PEI (Polysciences, USA) at a ratio of 1:2 (DNA:PEI). Plasmid DNA and PEI were diluted separately in HyCell TransFx-H in a volume corresponding to 2.5% of the volume of cells to be transfected. For experiments where the DNA was delivered on a volumetric basis, 1 μg of plasmid was added per milliliter of cell culture. For delivering DNA on a cell basis, 1 μg of plasmid was added per 10^6 viable cells. Diluted DNA and PEI were mixed and incubated at room temperature for 15 min. The DNA-PEI cocktail was then added to the cells.

2.4 | Determination of transfection efficiency

For evaluation of transfection efficiency, cells were collected 24 h post-transduction and fixed with a solution of 2% paraformaldehyde. Cells were analyzed using a BD Accuri C6 flow cytometer (BD Biosciences, USA), and EGFP expression was analyzed using BD Accuri C6 Plus Analysis Software (BD Biosciences, USA).

2.5 | Harvest of produced viral vectors

Viral particles (VPs) were harvested from the cell culture broth as previously described.[47,57] Briefly, the cells were harvested and lysed by adding a 10X Lysis Buffer (20 mM $MgCl_2$, 1% Triton X-100 in 500 mM Tris-buffered solution). Benzonase was added to a final concentration of 5 U mL^{-1} to digest host-cell DNA and unpacked virus DNA. After 1 h of incubation at 37°C with agitation, $MgSO_4$ was added to a final concentration of 37.5 mM to prevent AAV aggregation and binding to cellular components. After 30 min of incubation at 37°C with agitation, the lysate was clarified via centrifugation at 10,000 × *g* for 15 min. The clarified viral lysate was stored in a −80°C freezer.

2.6 | AAV production quantification

Genome-containing VPs were titrated via ddPCR.[58] Viral DNA from samples was extracted using a High Pure Viral Nucleic Acid Extraction kit (Roche Diagnostics, Switzerland). The following primers targeting the transgene were used: EGFP, 5′-CTGCTGCCCGACAACCAC-3′ (forward) and 5′-TCACGAACTCCAGCAGGAC-3′ (reverse); SaCas9, 5′-GGCCAGATTCAGGATGTGCT-3′ (forward) and 5′-CATCATCCCCAGAAGCGTGT-3′ (reverse). The primers were purchased from Integrated DNA Technologies (USA). The thermocycling temperature programming for EGFP was: preincubation at 95°C/15 min for denaturation. Forty cycles of 94°C/30 s, 53°C/30 s, and 72°C/1 min, and final extension at 72°C for 5 min. For SaCas9 was: preincubation at 95°C/15 min for denaturation. Forty cycles of 94°C/30 s, 60°C/1 min, and 72°C/30 s, and final extension at 72°C for 5 min. The plates were scanned on a QX100 droplet reader (Bio-Rad, USA), and the analysis was carried out with QuantaSoft software (Bio-Rad, USA). Quantification was performed as previously described[59] and the genomic titer was calculated as VG mL^{-1}. Cell-specific virus yield (CSVY) was determined by dividing the titer by the cell density at the time of harvest.

The total number of assembled capsids produced was quantified by enzyme-linked immunosorbent assay using the AAV6 ELISA Titration kit (Progen, Germany). Quantification was performed as per manufacturer's protocol and result was calculated as VP mL^{-1}.

2.7 | Functional virus titer via gene transfer assay

Suspension-adapted HEK293SF cells were transduced with serial dilutions of AAV6-GFP and co-infected with an E1, E3-deleted adenovirus serotype 5 (ΔE_1E_3Ad5) at an MOI of five infectious particles per cell. At 24 h post-transduction, the cells were harvested and fixed in 2% paraformaldehyde at 4°C for 30 min. Cells were analyzed using a BD Accuri C6 flow cytometer (BD Biosciences, USA), and EGFP expression was analyzed using BD Accuri C6 Plus Analysis Software (BD

Biosciences, USA). The linear range of quantification was established between 2% and 20% of GFP-positive cells.[60] The functional titer was calculated as enhanced transducing units (ETU) mL^{-1}.

2.8 | Analysis of medium nutrients and metabolites

Culture samples were collected every 24 h, centrifuged for removal of cell pellet, and the supernatant was analyzed in a BioProfile FLEX2 Analyzer (Nova Biomedical, USA) to determine the following nutrients and metabolites: glutamine, glutamic acid, glucose, lactate, and ammonium.

2.9 | Statistical analysis

Results are expressed as mean ± standard deviation. Student's *t*-test was used to measure the statistical significance between two groups. One-way analysis of variance (ANOVA) followed by Dunnett's post-hoc test was used to measure the statistical difference between three or more groups. $p < 0.05$ was considered to indicate a statistically significant difference. Asterisks are used to indicate p values as follows: $^{*}p < 0.05$, $^{**}p < 0.01$, $^{***}p < 0.005$, $^{****}p < 0.0005$.

3 | RESULTS

3.1 | Effect of plasmid DNA availability on AAV production at low cell densities

In the present study, we investigated the improvement of AAV6 production via transient transfection of suspension-adapted HEK293SF cells by increasing cell density. The standard AAV production in our laboratory is conducted via transfection at LCD with 1 μg of plasmid DNA per mL. First, we assessed if plasmid DNA availability played an important role during production in an increased cell density. We compared the AAV6 yield from productions at 1 and 2×10^6 cells mL^{-1}. During transfection, plasmid DNA was delivered either on a volumetric basis (1 μg mL^{-1}) or a cell basis (1 μg/10^6 cells). PEI concentration for all experiments was set at 2 μg per μg of plasmid DNA. Viral vectors were harvested 48 h post-transfection (hpt) to determine viral yield in terms of genome-containing particles (VG). The cell density and viability profiles during AAV production are shown in Figure 1A. Lower transduction efficiencies were observed in both productions at 2×10^6 cells mL^{-1} compared to the control (Figure 1B). A 2.4-fold increase in viral titer was observed in the transfection of 2×10^6 cells mL^{-1} when DNA was supplied on a cell basis (5.4×10^9 VG mL^{-1}), resulting in a better-than-linear increase of viral titer when compared to the standard production (2.2×10^9 VG mL^{-1}) (Figure 1C). Productions at 2×10^6 cells mL^{-1} showed the highest CSVY only when DNA was supplied on a cell basis (approximately 3100 VG $cell^{-1}$). The delivery of DNA as 1 μg mL^{-1} in the transfection of 2×10^6 cells mL^{-1} caused a reduction in the CSVY to only 870 VG $cell^{-1}$, resulting in a volumetric yield of only 1.8×10^9 VG mL^{-1}.

3.2 | Cell-specific production maintained at a medium cell density

The next step was to evaluate the viral vector production at an MCD (4×10^6 cells mL^{-1} at the time of transfection). To avoid detrimental effects from spent medium, the cells were inoculated at the desired concentration in fresh medium and transfected immediately. Again, the cells were transfected with plasmids on either a volumetric or cell basis and the viral titer VG mL^{-1} was assessed every 24 h. Figure 2A shows the cell density and viability profiles during AAV production at low and medium cell densities. A drop in the transfection efficiency was observed even when a higher amount of DNA was supplied (Figure 2C). However, as previously observed, this lower transfection efficiency did not impact viral titer (Figure 2B, DNA delivered on a cell basis). Similar to what was observed in the transfection of 2×10^6 cells mL^{-1}, the titer of the MCD production with DNA delivered on a cell basis (equivalent to 4 μg mL^{-1}) was 3.8 times the control, reaching 8.6×10^9 VG mL^{-1} (Figure 2B). DNA delivery on a volumetric basis resulted in 4.9×10^9 VG mL^{-1} (a 2.2-fold increase from the control). When DNA is supplied on a cell basis, the CSVY was maintained at around 1500 VG $cell^{-1}$. On the other hand, volumetric delivery of DNA resulted in a decrease to 600 VG $cell^{-1}$ (Figure 2B). The functional viral titers (enhanced transduction units (ETU) mL^{-1}) are summarized in Figure 2D. An increase in cell density resulted in a rise of functional titer by 2.5-3.9 times, depending on the harvest time. At 48 hpt, no statistically significant difference ($p = 0.4261$) was observed in the ratio VG/ETU between LCD and MCD production with 1 μg of DNA per 10^6 cells (Figure 2E). The total number of capsids produced was quantified by ELISA and the percentage of full capsids was calculated, resulting in a mean of 12.8% full capsids for LCD production and 29.8% full capsids for MCD production (ns, $p > 0.05$).

3.3 | The cell density effect was observed at higher density

To study if cell-based delivery of DNA would be enough to prevent the CDE at an HCD production, we evaluated AAV6 production at 10×10^6 cells mL^{-1}. A pseudo-perfusion was devised in 50-mL TubeSpin bioreactors to achieve the desired cell density. A working volume of 10 mL and medium exchange of 1 VVD were set. The medium exchange started 48 h after the seeding of the cells and was maintained past the transfection to keep providing fresh nutrients to the cells. Cells were transfected at a density of 10×10^6 cells mL^{-1}, with plasmid DNA delivered on a cell basis (equivalent to 10 μg mL^{-1}) and viral titer was assessed every 24 h. An LCD control was also prepared in similar vessels. As expected, the transduction of the high cell-density production was lower than the control (Figure 3A). Cell densities and

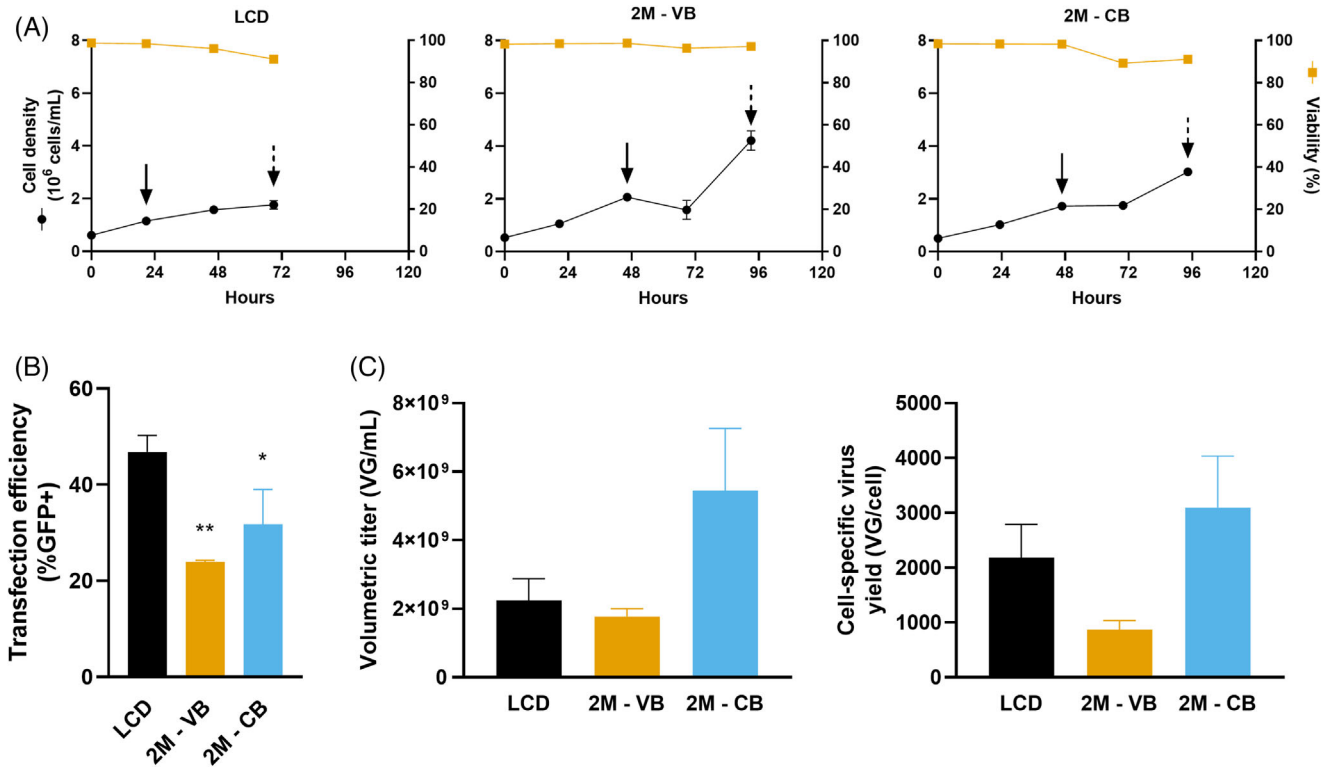

FIGURE 1 Production of adeno-associated virus 6 (AAV6) via triple transient transfection at low cell densities. Cells were transfected at 1×10^6 cells mL^{-1} (low cell density [LCD]) or 2×10^6 cells mL^{-1} (2M) in shake flasks, and plasmid DNA was delivered on a volumetric basis (VB: 1 μg mL^{-1}) or cell basis (CB: 1 $\mu g/10^6$ cells). (A) Cell growth kinetics and viability. Black arrows indicate the time of transfection, and dashed arrows indicate the time of viral harvest. (B) Transfection efficiency is described as the percentage of cells expressing the transgene (green fluorescent protein [GFP]) 24 h post-transfection. (C) Volumetric titer (viral genomes [VG] mL^{-1}) and cell-specific virus yields (VG $cell^{-1}$). Values represent mean ± standard deviation ($n = 3$). $^{**}p < 0.01$, $^{*}p < 0.05$, by analysis of variance (ANOVA) followed by Dunnett's test.

volumetric titers during AAV6 productions are shown in Figure 3B. AAV6 yield peaked at 72 hpt, and the HCD production resulted in 9.3 $\times 10^9$ VG mL^{-1}, a 4.6-fold increase compared to the LCD control. Even though the yield was higher than the control, this result shows that the titer does not increase linearly with the increase in cell density at the time of transfection. This difference becomes even more evident at the cell-specific level. At 72 hpt, the LCD batch control yielded an average of 1200 VG $cell^{-1}$, while the HCD pseudo-perfusion yielded less than 600 VG $cell^{-1}$ (Figure 5C).

3.4 | Medium supplementation improves cell-specific virus yield

Nutrients and cell metabolites were analyzed during the production of AAV6 at low and high cell densities in TubeSpin bioreactors. Even though the levels of metabolites (lactate and ammonium) would be maintained low, levels of glutamine and glutamic acid were kept constant by the medium exchange, a significant drop in glucose concentration was observed (Figures 4A,B). At 48 hpt, glucose concentration was 3.2 g L^{-1} (17.8 mM) for LCD, while for HCD, as low as 1.8 g L^{-1} (10 mM). Two other HCD productions were performed to evaluate the effect of medium supplementation. This time, the medium was supplemented with either glucose at a final concentration of 7.2 g L^{-1} (40 mM) or 15% Cell Boost 5, which resulted in a similar concentration of glucose between LCD and HCD production at their lowest points (Figure 4B).

Figure 5A shows the cell density and viability profiles during AAV6 production at HCD with basal and supplemented media, and Figure 5B shows the transfection efficiency 24 h post-transfection. Medium supplementation with Cell Boost 5 resulted in a higher growth rate after transfection, with cell density reaching 25.5×10^6 cells mL^{-1} 96 hpt, while cells in basal medium reached up to 20.4×10^6 cells mL^{-1}. Cells cultured in the glucose-supplemented medium showed a slower growth rate, resulting in the transfection being done one day later compared to the medium supplemented with Cell Boost 5. At 72 hpt, when compared to the use of the basal medium, the use of supplementation resulted in increased volumetric titer (1.4- and 1.6-fold increase for glucose and Cell Boost 5, respectively) and a significant improvement of CSVY (2.1-fold increase for Cell Boost 5) (Figure 5C). A mean of 25.5% full capsids were obtained at that timepoint.

Medium supplementation alleviated the observed CDE in the HCD production, resulting in CSVY similar to those in the LCD control, leading to an almost 10-fold increase in viral titer. There was an increase in functional titer when HCD production was supplemented. Cell-specific functional titer also increased depending on the supplementation, but

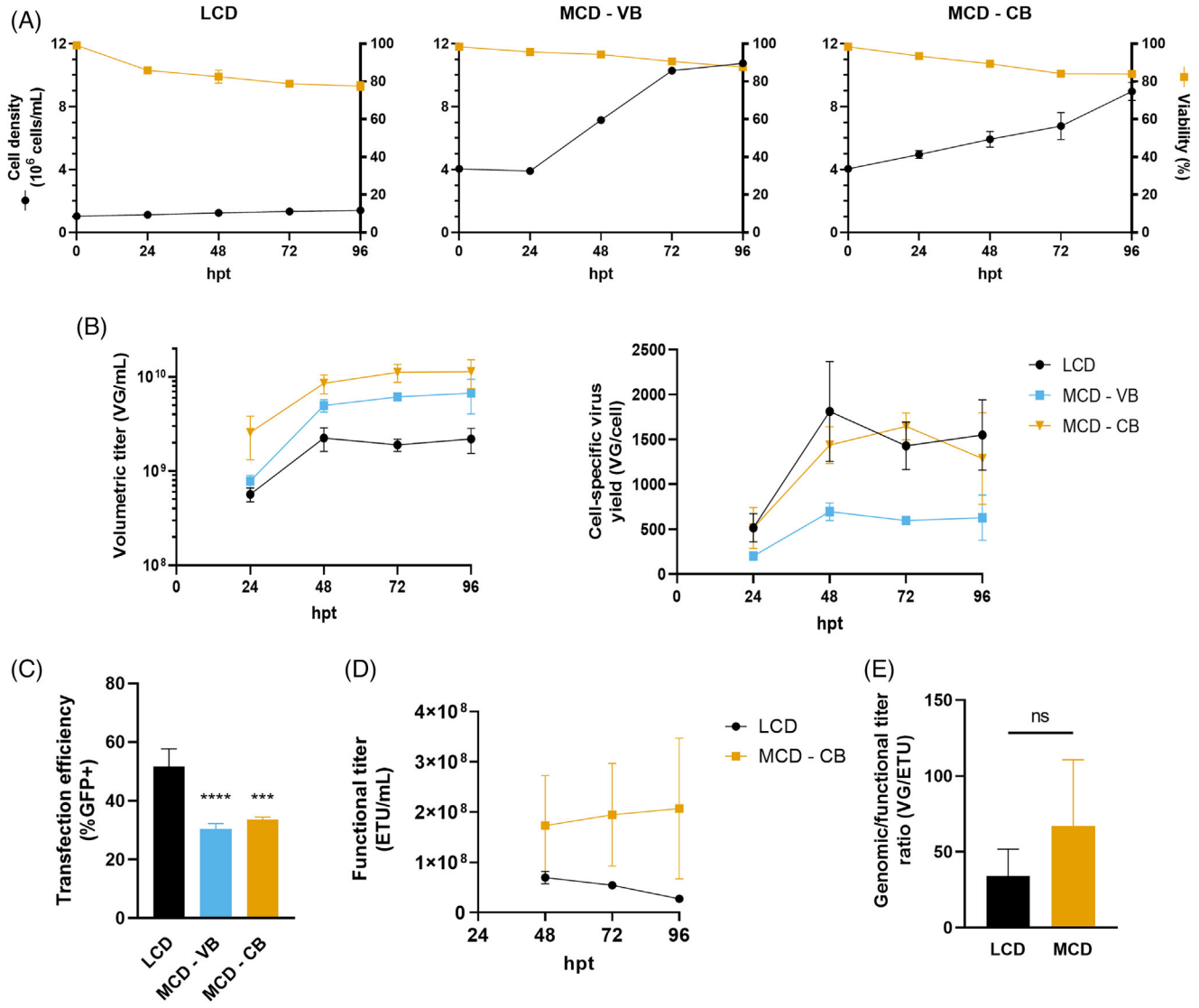

FIGURE 2 Production of adeno-associated virus 6 (AAV6) via triple transient transfection at medium cell densities. Cells were transfected at low cell density (LCD – 1×10^6 cells mL^{-1}) as control or at medium cell density (MCD – 4×10^6 cells mL^{-1}) in shake flasks. Plasmid DNA was delivered on a volumetric basis (VB: 1 μg mL^{-1}) or cell basis (CB: 1 $\mu g/10^6$ cells). (A) Cell growth kinetics and viability. (B) Volumetric (VG mL^{-1}) and cell-specific virus yields (viral genomes [VG] $cell^{-1}$). Time expressed in hours post-transfection (hpt). (C) Transfection efficiency is described as the percentage of cells expressing the transgene (green fluorescent protein [GFP]) 24 hpt (D) Functional titer (enhanced transducing units [ETU] mL^{-1}). (E) Ratio between the genomic titer and functional titer (VG/ETU) 48 hpt, the lower the better. Values represent mean ± standard deviation ($n = 2$). ****$p < 0.0001$, ***$p < 0.001$, by analysis of variance (ANOVA) followed by Dunnett's test and Student's *t*-test.

it was two times inferior compared to the LCD (Figure 6A). The VG/ETU ratio for LCD production was 34.4, while for HCD, it reached 79.9 when the medium was supplemented with Cell Boost 5 (Figure 6B).

3.5 | Validation of medium cell density production at bioreactor scale

Since the MCD production resulted in a significant improvement in titer and no loss in functionality, we decided to evaluate the scalability of this process. For that, we conducted the production in a 3-L bioreactor, where the cells were seeded at 4×10^6 cells mL^{-1} in fresh medium and were immediately transfected with plasmids delivered on a cell basis. Whole broth culture was sampled at 8–16 h intervals. A satellite culture, with a volume of around 25 mL taken from the bioreactor post-transfection, was evaluated in parallel in a shake flask (Figure S1). At 24 hpt, a transfection efficiency of 36.9% was observed, similar to the production in shake flasks (33.8%, Figure 2C). Figure 7 shows cellular and production kinetics in the bioreactor, demonstrating that MCD production is feasible at a bioreactor scale. LCD 3-L bioreactor productions previously completed in our laboratory were used as control. In these LCD runs, AAV6 vectors packaging a genome without fluorescent marker were produced; thus, it was impractical to assess their functional titer. Cell density in the MCD bioreactor reached its maximum

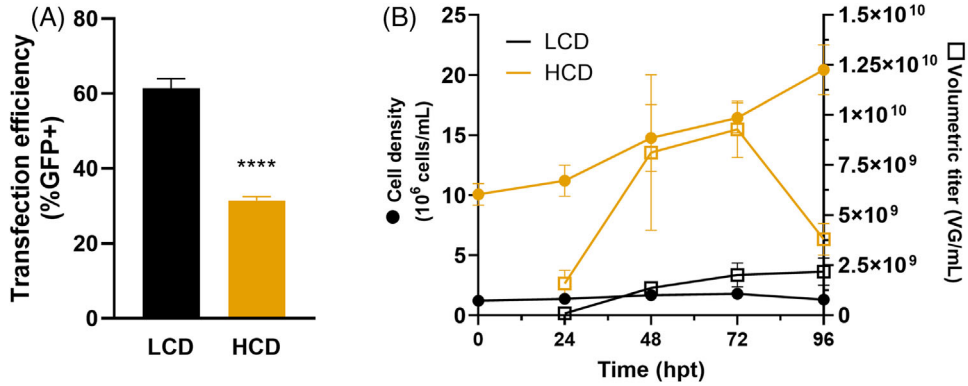

FIGURE 3 Production of adeno-associated virus 6 (AAV6) via triple transient transfection at high cell density. Cells were transfected at low cell density (LCD – 1×10^6 cells mL^{-1}) as control or at high cell density (HCD – 10×10^6 cells mL^{-1}) in TubeSpin bioreactors. Plasmid DNA was delivered on a cell basis (1 $\mu g/10^6$ cells). (A) transfection efficiency is described as the percentage of cells expressing the transgene (green fluorescent protein [GFP]) 24 h post-transfection. (B) Cell growth kinetics (●) and volumetric viral yield (□). Values represent mean ± standard deviation ($n = 3$). ***$p < 0.001$, by Student's *t*-test.

at 59 hpt with 9.5×10^6 viable cells mL^{-1}. Vector production peaked around 60 hpt with a titer of 5.9×10^{10} VG mL^{-1}, an ~4-fold increase compared to control bioreactors (Figure 7C), with 22.2% full capsids. The CSVY was around 6000 VG $cell^{-1}$, similar to the LCD production in bioreactors (Figure 7D). Regarding the functional titer, the bioreactor yielded 7.8×10^9 ETU mL^{-1} 48 h post-transfection (Figure 7E). As a result, the VG/ETU ratio was as low as 4.6 at 48 hpt, plateauing around 10 at subsequent time points (Figure 7F).

4 | DISCUSSION

In Figure 1, we observe that plasmid DNA availability plays an essential role in the maintenance of VG titer when cell density at the time of transfection is increased from 1 to 2×10^6 cells mL^{-1}. In LCD transient transfection, plasmid DNA is usually delivered on a volumetric basis.[45,47–50] Like our study, Grieger et al.[48] also observed a titer increase during production when cell density and plasmid concentration were doubled. The need for a higher plasmid DNA concentration was also observed for productions at 4×10^6 cells mL^{-1} (MCD). A four-fold increase in the number of cells at the time of transfection resulted in an almost linear increase in viral titer (VG mL^{-1}) only when plasmid DNA was delivered per 10^6 cells (Figure 2B). Moreover, the CSVY was maintained during MCD production, with plasmid DNA concentration maintained on a per-cell basis (Figure 2B). Yields around 1500 VG $cell^{-1}$ were obtained, similar to those reported by Chahal et al.[47] The improvement in titer was also observed for functional particles (ETU). The functional titer of the MCD production with plasmid DNA delivered on a cell basis was maintained constant (Figure 2D), resulting in a difference of up to 3.9 times compared to the LCD control at 96 hpt. At LCD, the slight decrease in transducing units, but not in genome-containing particles, could be explained by the loss in functionality of the viral vectors. AAV vectors are thermally stable, but their transduction efficiency decreases when maintained at 37°C and as the pH decreases.[61] Extending the culture to 96 hpt can decrease intracellular and extracellular pH due to the accumulation of metabolites, such as ammonia and lactate.[62,63]

The VG/ETU ratio measures viral functionality, showing the proportion of genome-containing viruses competent to transduce a target cell. At 48 hpt, the MCD production had a mean VG/ETU ratio of 67.1 (Figure 2E). Although this value is higher than reported in the literature,[47,48] there was no statistically significant difference from our LCD control. As shown in Figure 7, the production of AAV6 at MCD was successfully performed at a 3-L bioreactor. The cells were inoculated into the bioreactor in fresh medium at the desired cell density of 4×10^6 cells mL^{-1} to prevent detrimental effects from the spent medium. At larger scales, this could be achieved, for example, by medium exchange using a membrane-based cell retention device, such as the alternating tangential flow (ATF) or the tangential flow depth filtration (TFDF) system.[64,65] This bioreactor production resulted in 30-fold increase in VG mL^{-1} titer, compared to previously reported production at a similar scale.[47] Surprisingly, the viral vector yield on the bioreactor was around 10-fold higher than the small-scale satellite culture. Similarly, the LCD bioreactor production also showed a higher yield than the small-scale experiments. This enhanced production in the bioreactors could be associated with better-regulated culture conditions, such as DO and pH. Again, no loss in functional titer was observed, with a maximum value of 7.8×10^9 ETU mL^{-1} achieved 48 h post-transfection and a VG/ETU ratio of 4.6 (Figure 7D,E). These results show an improvement from previous reports.[47,48]

When productions were conducted at cell densities other than 1×10^6 cell mL^{-1}, the transfection efficiency, measured by the expression of the transgene 24 h post-transfection, decreased to about 30% independently of the cell density (Figure 1B, Figure 2C, and Figure 3A). However, the percentage of cells expressing the transgene did not correlate directly with production efficiency. Others observed this same phenomenon during the production of viral-like particles via transient transfection of HEK293SF suspension cells.[66] Hildinger et al.[67]

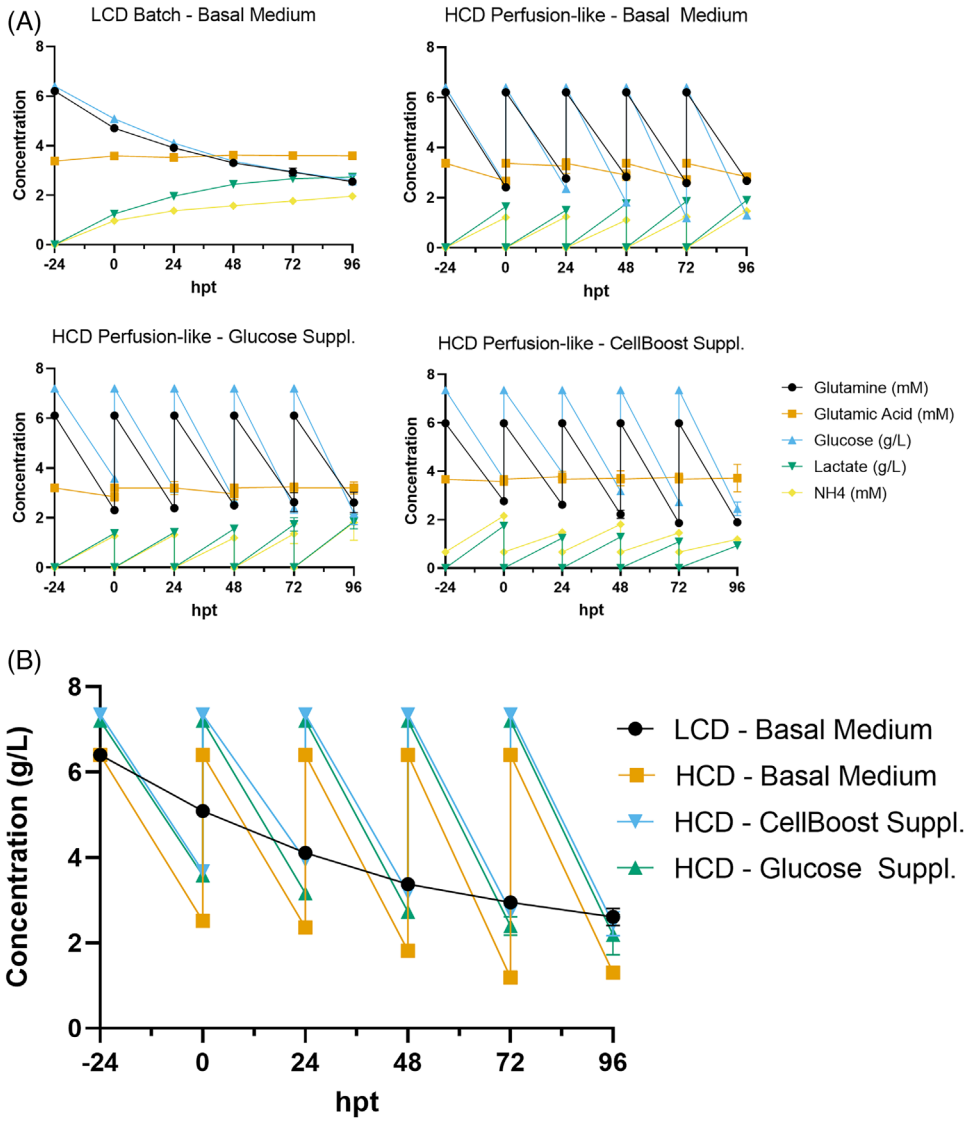

FIGURE 4 Metabolite profiles of production of adeno-associated virus 6 (AAV6) via triple transient transfection at high cell density. Cells were transfected at low cell density (LCD – 1×10^6 cells mL^{-1}) as control or at high cell density (HCD – 10×10^6 cells mL^{-1}) in TubeSpin bioreactors. Plasmid DNA was delivered on a cell basis (1 $\mu g/10^6$ cells). (A) Nutrient and metabolite concentrations for production at low and high cell densities using basal or supplemented medium (7.2 g L^{-1} [40 mM] glucose concentration or 15% Cell Boost 5). (B) Concentration of glucose for productions at low and high cell densities. Values represent mean ± standard deviation ($n = 3$).

concluded that the transfection efficiency reduction resulted from DNA being provided on a volumetric basis. However, increasing the plasmid DNA availability in our study did not significantly improve transduction efficiency (Figure 1B, Figure 2C, and Figure 3A), as measured by the detection of the product of one of the three plasmids, which corroborates previous findings.[47] Increased energetic demand is reported to occur at higher cell densities and to allow recovery from transfection, an event known to be cytotoxic.[68] Transfection efficiency did not improve during production in pseudo-perfusion, even when the medium was supplemented (Figure 5B). The transfection efficiency was even lower at a higher glucose concentration. Lavado-García et al.[68] partially explained the low transfection efficiency as a result of downregulated pathways involved in lipid biosynthesis and nuclear transportation of intracellular proteins. The transfection step, per se, is a known bottleneck in the production of AAV vectors. A recent study from our group showed that the proportion of cells that produce VPs is as low as 7%, despite high transduction efficiency.[69]

Recently, the improvement of AAV8 production at high-cell density with a medium exchange strategy was reported.[65] Conversely, the CDE was confirmed during our HCD productions (Figures 3B and 5). CDE refers to the diminished production at high cell densities resulting from decreased cell-specific productivity.[55,70] This effect has been previously documented for the generation of AAV using other production systems, such as insect cells.[53,60,71–73] During production, 25–30% of the AVV6 vectors are released in the supernatant.[47] Because of the HCD and the elevated shaking speed to properly oxygenate the bioreactors used, it is possible that the cells were under increased sheer stress and could have released more vectors into the

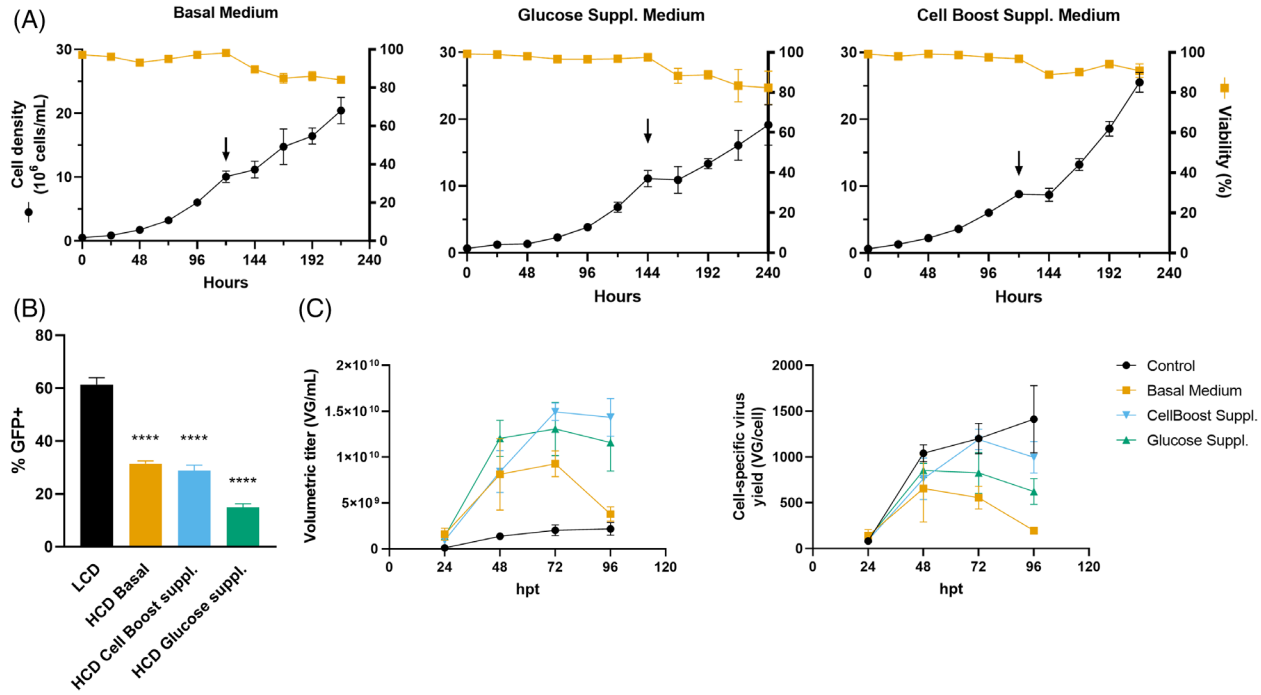

FIGURE 5 Effect of medium supplementation on the production of adeno-associated virus 6 (AAV6) at high cell density (HCD). HyCell TransFx-H (basal medium) was supplemented with glucose (7.2 g L^{-1} [40 mM] final concentration) or with 15% Cell Boost 5. (A) Cell growth kinetics and viability. Black arrows indicate the time of transfection. (B) Transfection efficiency is described as the percentage of cells expressing the transgene (green fluorescent protein [GFP]) 24 h post-transfection (hpt). (C) Volumetric (viral genomes [VG] mL^{-1}) and cell-specific virus yields (VG $cell^{-1}$) of low cell-density control and high cell-density productions with basal and supplemented media. Experiment conducted in TubeSpin bioreactors. Data from Figure 3 for the group HCD has been replotted here as Basal Medium. Values represent mean ± standard deviation ($n = 3$).

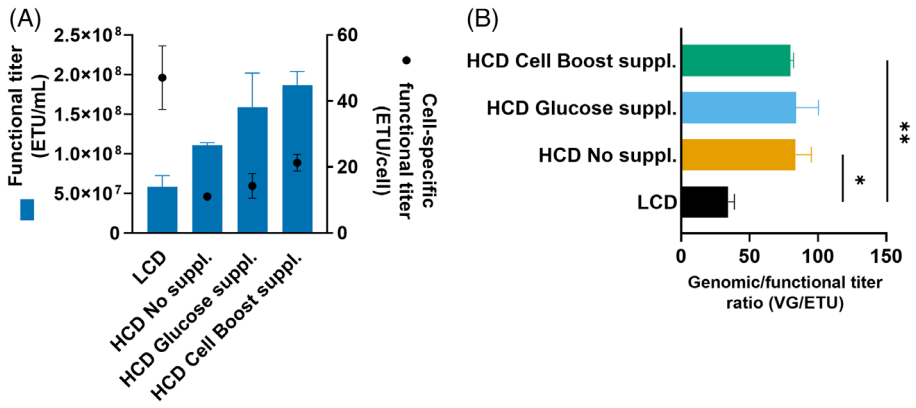

FIGURE 6 Effect of medium supplementation of functional titers of adeno-associated virus 6 (AAV6) produced at high cell density. (A) Functional titer (enhanced transducing units [ETU] mL^{-1}) and cell-specific functional titer (ETU mL^{-1}) at 72 hpt. (B) Ratio between volumetric and functional titer at 72 hpt. Experiment conducted in TubeSpin bioreactors. HCD, high cell density; LCD, low cell density control. Values represent mean ± standard deviation ($n = 3$). $^{**}p < 0.01$, $^{*}p < 0.05$, by analysis of variance (ANOVA) followed by Dunnett's test.

supernatant, which were removed during the medium exchange. This could explain the sudden drop in viral titer at 96 hpt in the HCD production (Figure 3B), which is not expected since AAV vectors are considered very stable at a wide range of temperatures.[61,74] The same drop, however, was not observed when the medium was supplemented (Figure 5C).

The CDE is thought to occur mainly due to metabolic limitations caused by low concentrations of nutrients or the accumulation of inhibitory metabolites.[53,55,75] During the production at HCD, a pseudo-perfusion was employed to provide enough nutrients to support HCD and remove inhibitory metabolites; however, the conditions selected were insufficient to prevent the CDE (Figure 3). The glucose

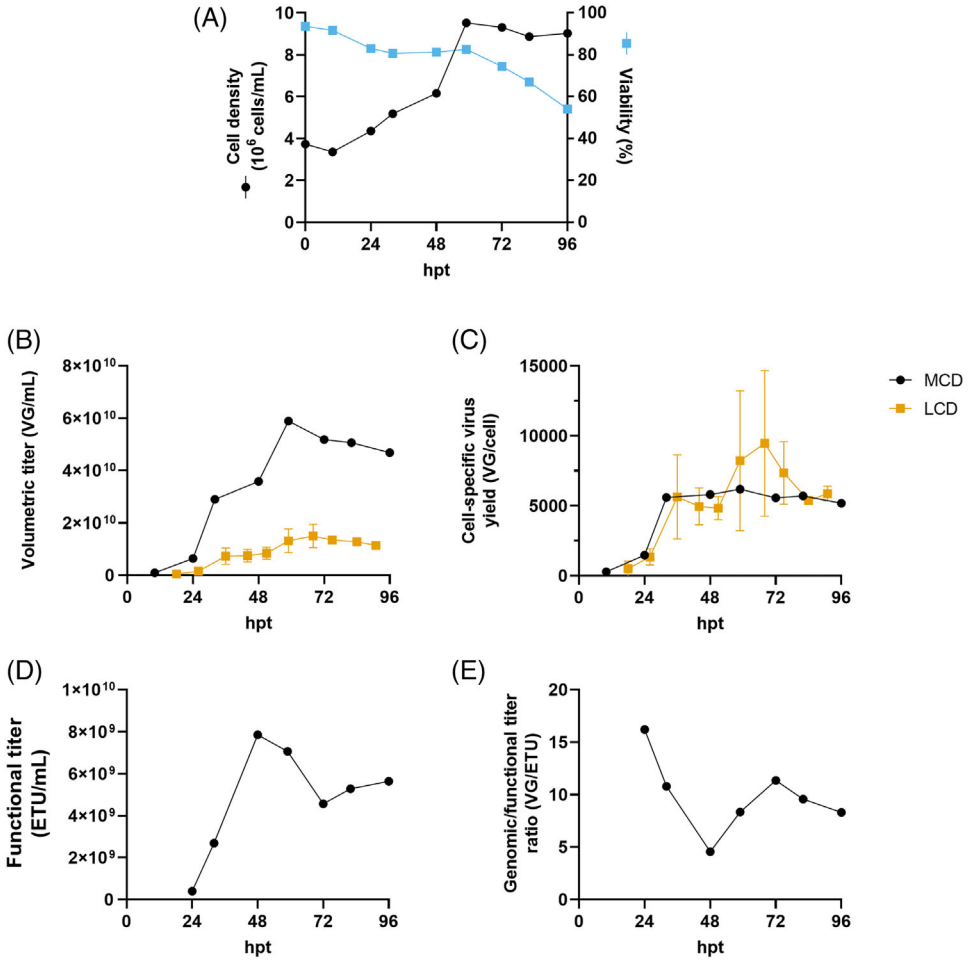

FIGURE 7 3-L bioreactor production of adeno-associated virus 6 (AAV6) at medium cell density. Cells were transfected at 4×10^6 cells mL^{-1} (medium cell density [MCD]), and plasmid DNA was delivered on a cell basis ($1\ \mu g/10^6$ cells). Low cell density (LCD, 1×10^6 cell mL^{-1}) 3-L bioreactor productions from previous runs (unpublished data) shown as control. (A) Cell growth kinetics and viability for MCD production. (B) Volumetric titer (viral genomes [VG] mL^{-1}). (C) Cell-specific virus yield (VG/cell). (D) Functional titer (enhanced transducing units [ETU] mL^{-1}). (E) Ratio between genomic and functional titer (VG/ETU). Values represent mean ± standard deviation ($n = 1$ for MCD; $n = 2$ for LCD).

level dropped significantly at HCD, even though the medium was fully exchanged daily. For that reason, the basal medium, HyCell TransFx-H, which contains around 6 g L^{-1} (33.3 mM) of glucose, was supplemented with either glucose or Cells Boost 5. The amount of supplement added was based on the cell-specific consumption rate of glucose (average of 4.8 pmol $cell^{-1}$ day^{-1} and similar to reported values[76]) so that a minimum of 2 g L^{-1} (11.1 mM) of glucose was available at any given time,[77] mimicking the observed glucose concentrations in the LCD productions. HEK293 cells exhibit a high level of glycolytic activity[78] and higher consumption rates have been associated with improved viral productions.[79] Medium supplementation with glucose alone only partially restored the CSVY of AAV6 (Figure 5C). The CDE was alleviated, and the CSVY was restored to LCD levels when a medium supplemented with 15% Cell Boost 5 was used (Figure 5C), indicating that other critical nutrients were limiting viral vector yield. Besides glucose, other components of the Cell Boost 5 supplement are thought to contribute to alleviating the CDE. While producing adenoviral vectors using the HEK293SF cells, Shen et al.[80] emphasized that the composition of the medium used is crucial to support high yields at HCD. However, the complexity of culture media and supplements, such as Cell Boost 5, which can contain hundreds of different components at variable concentrations, complicates the understanding of individual nutrients' effect on viral vector productions.[55] An optimized cell culture medium to produce AAV vectors could improve titers and vector quality, as seen and suggested for other viral vectors[62,68,77,80]

As discussed above, supplementing the medium with Cell Boost 5 alleviated the CDE in terms of genome-containing particles; however, the same was not observed for functional particles. Whereas there was an increase in functional yield when the medium was supplemented, the cell-specific functional titer (ETU/cell) was not fully maintained, resulting in higher VG/ETU ratios compared to the LCD control (Figure 6). One possible explanation is the misassembly of the viral capsid, which contains a stoichiometry of 1:1:10 (VP1:VP2:VP3). If this proportion is altered, the efficacy of the AAV to deliver the transgene decreases.[81] Due to nuclear localization signals, the VP1 and VP2 proteins play a crucial role in transduction, specifically in nuclear

transportation.[82] The N-terminus of VP1 also contains a phospholipase A2 domain responsible for viral escape from the endosome.[83–86] Our results highlight the importance of assessing viral transduction efficacy by measuring biologically active vectors[87] as part of optimizing AAV vector production. This measurement is sometimes overlooked by authors,[49,51] even though the quality attributes of a viral vector, including functional titer, are an essential part of the potency tests recommended by the FDA.[88] In order to find a solution to the issue of decreased virus functionality at HCD, future studies could, for instance, further research the effects of medium composition or evaluate alternative modes of operation, such as fed-batch. One crucial aspect that should be evaluated during viral vector production is the percentage of capsids that contain the genome. The presence of empty particles, which lack the transgene cargo, can significantly compromise the transduction efficiency of the vector.[89] Additionally, when used in vivo, empty capsids can induce innate and adaptative immune responses.[90] No significant difference was observed in the percentage of full capsids between LCD and MCD methods. In fact, the MCD production resulted in a slightly higher percentage compared to the LCD control. Nevertheless, it is possible to further enhance this metric via purification using anion-exchange chromatography. This technique can aid in the separation and isolation of full capsids from partial or empty ones, ultimately leading to a higher yield of functional vectors.[57]

In summary, we demonstrated that it is possible to produce AAV6 via triple transient transfection at MCD in fresh medium without losing cell-specific productivity or functional titer. For that, the plasmid DNA must be provided on a cell basis. Our MCD productions achieved titers at the order of 10^{10} VG mL^{-1} of crude lysate. The yields obtained by this method represent a significant increase compared to a well-established production protocol.[47] The MCD method for AAV vector production described in this manuscript was shown to be efficient at a 3-L bioreactor scale. It could be used as the foundation for large-scale production processes, potentially contributing to solving the current vector shortage in AAV manufacturing. The authors are aware that this method can be associated with high manufacturing costs due to the significant quantity of plasmid DNA required[49,91] and that further development of plasmid production systems are needed. The CDE could be alleviated at a higher cell density, resulting in similar CSVY (VG/cell) when a pseudo-perfusion was conducted with a supplemented medium. However, the cell-specific functional productivity (ETU/cell) was reduced, highlighting the importance of evaluating both VG and transducing units during bioprocess optimization. Further research is necessary to fully understand how the CDE results in reduced functional titer and how to alleviate it fully.

AUTHOR CONTRIBUTIONS

Conceptualization: Pablo D. Moço, Amine A. Kamen; Investigation: Pablo D. Moço, Xingge Xu; Formal analysis: Pablo D. Moço, Cristina A. T. Silva; Writing – original draft: Pablo D. Moço; Writing – review & editing: Pablo D. Moço, Xingge Xu, Cristina A. T. Silva, Amine A. Kamen; Supervision: Amine A. Kamen, Funding acquisition: Amine A. Kamen.

ACKNOWLEDGMENTS

Pablo D. Moço is financially supported by a fellowship from the Faculty of Engineering at McGill University and a doctoral scholarship from the Fonds de Recherche du Québec – Santé (FRQS). Xingge Xu is financially supported by a doctoral scholarship from Fonds de Recherche du Québec – Nature et technologies (FRQNT). Amine A. Kamen is partially funded through Canada Research Chair CRC-240394. The funding sources were not involved in the study design, the collection, analysis and interpretation of data, the writing of the report or the decision to submit the article for publication.

CONFLICT OF INTEREST STATEMENT

The authors declare that they have no known competing financial interests or personal relationships that could have appeared to influence the work reported in this paper.

DATA AVAILABILITY STATEMENT

The data that support the findings of this study are available from the corresponding author upon reasonable request.

REFERENCES

1. Georg-Fries, B., Biederlack, S., Wolf, J., & zur Hausen, H. (1984). Analysis of proteins, helper dependence, and seroepidemiology of a new human parvovirus. *Virology*, *134*, 64–71.
2. Atchison, R. W., Casto, B. C., & Hammon, W. M. (1965). Adenovirus-associated defective virus particles. *Science*, *149*, 754–756.
3. Hoggan, M. D., Blacklow, N. R., & Rowe, W. P. (1966). Studies of small DNA viruses found in various adenovirus preparations: Physical, biological, and immunological characteristics. *Proceedings of the National Academy of Sciences of the United States of America*, *55*, 1467–1474.
4. European Medicines Agency. (2012). Assessment Report: Glybera. https://www.ema.europa.eu/en/medicines/human/EPAR/glybera
5. U. S. (2017). Food and Drug Administration. Luxturna BL 125610/0 Approval Letter. https://www.fda.gov/vaccines-blood-biologics/cellular-gene-therapy-products/luxturna
6. U. S. (2019). Food and Drug Administration, Zolgensma BL. 125694/0 Approval Letter. https://www.fda.gov/vaccines-blood-biologics/zolgensma
7. Parks, W. P., Melnick, J. L., Rongey, R., & Mayor, H. D. (1967). Physical assay and growth cycle studies of a defective adeno-satellite virus. *Journal of Virology*, *1*, 171–180.
8. Bantel-Schaal, U., & Zur Hausen, H. (1984). Characterization of the DNA of a defective human parvovirus isolated from a genital site. *Virology*, *134*, 52–63.
9. Rutledge, E. A., Halbert, C. L., & Russell, D. W. (1998). Infectious clones and vectors derived from adeno-associated virus (AAV) serotypes other than AAV Type 2. *Journal of Virology*, *72*, 309–319.
10. Gao, G. P., Alvira, M. R., Wang, L., Calcedo, R., Johnston, J., & Wilson, J. M. (2002). Novel adeno-associated viruses from rhesus monkeys as vectors for human gene therapy. *Proceedings of the National Academy of Sciences of the United States of America*, *99*, 11854–11859.
11. Gao, G., Vandenberghe, L. H., Alvira, M. R., Lu, Y., Calcedo, R., Zhou, X., & Wilson, J. M. (2004). Clades of adeno-associated viruses are widely disseminated in human tissues. *Journal of Virology*, *78*, 6381–6388.
12. Mori, S., Wang, L., Takeuchi, T., & Kanda, T. (2004). Two novel adeno-associated viruses from cynomolgus monkey: Pseudotyping characterization of capsid protein. *Virology*, *330*, 375–383.
13. Schmidt, M., Voutetakis, A., Afione, S., Zheng, C., Mandikian, D., & Chiorini, J. A. (2008). Adeno-associated virus type 12 (AAV12): A

novel AAV serotype with sialic acid- and heparan sulfate proteoglycan-independent transduction activity. *Journal of Virology*, *82*, 1399–1406.
14. Schmidt, M., Govindasamy, L., Afione, S., Kaludov, N., Agbandje-McKenna, M., & Chiorini, J. A. (2008). Molecular characterization of the heparin-dependent transduction domain on the capsid of a novel adeno-associated virus isolate, AAV(VR-942). *Journal of Virology*, *82*, 8911–8916.
15. Srivastava, A. (2016). In vivo tissue-tropism of adeno-associated viral vectors. *Current Opinion in Virology*, *21*, 75–80.
16. Schober, A. L., Gagarkin, D. A., Chen, Y., Gao, G., Jacobson, L., & Mongin, A. A. (2016). Recombinant adeno-associated virus serotype 6 (rAAV6) potently and preferentially transduces rat astrocytes in vitro and in vivo. *Frontiers in Cellular Neuroscience*, *10*, 262.
17. Sayroo, R., Nolasco, D., Yin, Z., Colon-Cortes, Y., Pandya, M., Ling, C., & Aslanidi, G. (2016). Development of novel AAV serotype 6 based vectors with selective tropism for human cancer cells. *Gene Therapy*, *23*, 18–25.
18. Sheppard, H. M., Ussher, J. E., Verdon, D., Chen, J., Taylor, J. A., & Dunbar, P. R. (2013). Recombinant adeno-associated virus serotype 6 efficiently transduces primary human melanocytes. *PLoS ONE*, *8*, e62753.
19. Blankinship, M. J., Gregorevic, P., Allen, J. M., Harper, S. Q., Harper, H., Halbert, C. L., Miller, D. A., & Chamberlain, J. S. (2004). Efficient transduction of skeletal muscle using vectors based on adeno-associated virus serotype 6. *Molecular Therapy*, *10*, 671–678.
20. Wang, Z., Kuhr, C. S., Allen, J. M., Blankinship, M., Gregorevic, P., Chamberlain, J. S., Tapscott, S. J., & Storb, R. (2007). Sustained AAV-mediated dystrophin expression in a canine model of duchenne muscular dystrophy with a brief course of immunosuppression. *Molecular Therapy*, *15*, 1160–1166.
21. Qiao, C., Zhang, W., Yuan, Z., Shin, J. H., Li, J., Jayandharan, G. R., Zhong, L., Srivastava, A., Xiao, X., & Duan, D. (2010). Adeno-associated virus serotype 6 capsid tyrosine-to-phenylalanine mutations improve gene transfer to skeletal muscle. *Human Gene Therapy*, *21*, 1343–1348.
22. Palomeque, J., Chemaly, E. R., Colosi, P., Wellman, J. A., Zhou, S., Del Monte, F., & Hajjar, R. J. (2007). Efficiency of eight different AAV serotypes in transducing rat myocardium in vivo. *Gene Therapy*, *14*, 989–997.
23. Raake, P. W., Hinkel, R., Müller, S., Delker, S., Kreuzpointner, R., Kupatt, C., Katus, H. A., Kleinschmidt, J. A., Boekstegers, P., & Müller, O. J. (2008). Cardio-specific long-term gene expression in a porcine model after selective pressure-regulated retroinfusion of adeno-associated viral (AAV) vectors. *Gene Therapy*, *15*, 12–17.
24. White, J. D., Thesier, D. M., Swain, J. B. D., Katz, M. G., Tomasulo, C., Henderson, A., Wang, L., Yarnall, C., Fargnoli, A., Sumaroka, M., Isidro, A., Petrov, M., Holt, D., Nolen-Walston, R., Koch, W. J., Stedman, H. H., Rabinowitz, J., & Bridges, C. R. (2011). Myocardial gene delivery using molecular cardiac surgery with recombinant adeno-associated virus vectors in vivo. *Gene Therapy*, *18*, 546–552.
25. van Lieshout, L. P., Domm, J. M., Rindler, T. N., Frost, K. L., Sorensen, D. L., Medina, S. J., Booth, S. A., Bridges, J. P., & Wootton, S. K. (2018). A novel triple-mutant AAV6 capsid induces rapid and potent transgene expression in the muscle and respiratory tract of mice. *Molecular Therapy – Methods & Clinical Development*, *9*, 323–329.
26. Sharma, A., Ghosh, A., Hansen, E. T., Newman, J. M., & Mohan, R. R. (2010). Transduction efficiency of AAV 2/6, 2/8 and 2/9 vectors for delivering genes in human corneal fibroblasts. *Brain Research Bulletin*, *81*, 273–278.
27. Wang, J., DeClercq, J. J., Hayward, S. B., Li, P. W., Shivak, D. A., Gregory, P. D., Lee, G., & Holmes, M. C. (2015). Highly efficient homology-driven genome editing in human T cells by combining zinc-finger nuclease mRNA and AAV6 donor delivery. *Nucleic Acids Research*, *44*, e30.
28. Rogers, G. L., Huang, C., Clark, R. D. E., Seclén, E., Chen, H.-Y., & Cannon, P. M. (2021). Optimization of AAV6 transduction enhances site-specific genome editing of primary human lymphocytes. *Molecular Therapy – Methods & Clinical Development*, *23*, 198–209.
29. Nawaz, W., Huang, B., Xu, S., Li, Y., Zhu, L., Yiqiao, H., Wu, Z., & Wu, X. (2021). AAV-mediated in vivo CAR gene therapy for targeting human T-cell leukemia. *Blood Cancer Journal*, *11*, 119.
30. Sather, B. D., Romano Ibarra, G. S., Sommer, K., Curinga, G., Hale, M., Khan, I. F., Singh, S., Song, Y., Gwiazda, K., Sahni, J., Jarjour, J., Astrakhan, A., Wagner, T. A., Scharenberg, A. M., & Rawlings, D. J. (2015). Efficient modification of CCR5 in primary human hematopoietic cells using a megaTAL nuclease and AAV donor template. *Science Translational Medicine*, *7*, 307ra156.
31. Hale, M., Lee, B., Honaker, Y., Leung, W. H., Grier, A. E., Jacobs, H. M., Sommer, K., Sahni, J., Jackson, S. W., Scharenberg, A. M., Astrakhan, A., & Rawlings, D. J. (2017). Homology-directed recombination for enhanced engineering of chimeric antigen receptor T cells. *Molecular Therapy – Methods & Clinical Development*, *4*, 192–203.
32. MacLeod, D. T., Antony, J., Martin, A. J., Moser, R. J., Hekele, A., Wetzel, K. J., Brown, A. E., Triggiano, M. A., Hux, J. A., Pham, C. D., Bartsevich, V. V., Turner, C. A., Lape, J., Kirkland, S., Beard, C. W., Smith, J., Hirsch, M. L., Nicholson, M. G., Jantz, D., … McCreedy, B. (2017). Integration of a CD19 CAR into the TCR alpha chain locus streamlines production of allogeneic gene-edited CAR T cells. *Molecular Therapy*, *25*, 949–961.
33. Eyquem, J., Mansilla-Soto, J., Giavridis, T., van der Stegen, S. J., Hamieh, M., Cunanan, K. M., Odak, A., Gonen, M., & Sadelain, M. (2017). Targeting a CAR to the TRAC locus with CRISPR/Cas9 enhances tumour rejection. *Nature*, *543*, 113–117.
34. Dai, X., Park, J. J., Du, Y., Kim, H. R., Wang, G., Errami, Y., & Chen, S. (2019). One-step generation of modular CAR-T cells with AAV–Cpf1. *Nature Methods*, *16*, 247–254.
35. Moço, P. D., Aharony, N., & Kamen, A. (2020). Adeno-associated viral vectors for homology-directed generation of CAR-T cells. *Biotechnology Journal*, *15*, 1900286.
36. Naeimi Kararoudi, M., Likhite, S., Elmas, E., Yamamoto, K., Schwartz, M., Sorathia, K., de Souza Fernandes Pereira, M., Sezgin, Y., Devine, R. D., Lyberger, J. M., Behbehani, G. K., Chakravarti, N., Moriarity, B. S., Meyer, K., & Lee, D. A (2022). Optimization and validation of CAR transduction into human primary NK cells using CRISPR and AAV. *Cell Reports Methods*, *2*(6), 100236.
37. ClinicalTrials.gov, AAV (2022). from https://clinicaltrials.gov/ct2/results/browse?term=AAV&brwse=cond_alpha_all
38. Au, H. K. E., Isalan, M., & Mielcarek, M. (2022). Gene therapy advances: A meta-analysis of AAV usage in clinical settings. *Frontiers of Medicine*, *8*, 809118.
39. Grimm, D., Kern, A., Rittner, K., & Kleinschmidt, J. A. (1998). Novel tools for production and purification of recombinant adenoassociated virus vectors. *Human Gene Therapy*, *9*, 2745–2760.
40. Xiao, X., Li, J., & Samulski, R. J. (1998). Production of high-titer recombinant adeno-associated virus vectors in the absence of helper adenovirus. *Journal of Virology*, *72*, 2224–2232.
41. Collaco, R. F., Cao, X., & Trempe, J. P. (1999). A helper virus-free packaging system for recombinant adeno-associated virus vectors. *Gene*, *238*, 397–405.
42. Matsushita, T., Elliger, S., Elliger, C., Podsakoff, G., Villarreal, L., Kurtzman, G., Iwaki, Y., & Colosi, P. (1998). Adeno-associated virus vectors can be efficiently produced without helper virus. *Gene Therapy*, *5*, 938–945.
43. Wright, J. F. (2009). Transient transfection methods for clinical adeno-associated viral vector production. *Human gene Therapy*, *20*, 698–706.
44. Salabarria, S. M., Nair, J., Clement, N., Smith, B. K., Raben, N., Fuller, D. D., Byrne, B. J., & Corti, M. (2020). Advancements in AAV-mediated gene therapy for pompe disease. *Journal of Neuromuscular Diseases*, *7*, 15–31.

45. Park, J. Y., Lim, B. P., Lee, K., Kim, Y. G., & Jo, E. C. (2006). Scalable production of adeno-associated virus type 2 vectors via suspension transfection. *Biotechnology and Bioengineering*, *94*, 416–430.
46. Smith, J., Grieger, J., & Samulski, R. J. (2018). Overcoming bottlenecks in AAV manufacturing for gene therapy. *Cell and Gene Therapy Insights*, *4*, 815–825.
47. Chahal, P. S., Schulze, E., Tran, R., Montes, J., & Kamen, A. A. (2014). Production of adeno-associated virus (AAV) serotypes by transient transfection of HEK293 cell suspension cultures for gene delivery. *Journal of Virological Methods*, *196*, 163–173.
48. Grieger, J. C., Soltys, S. M., & Samulski, R. J. (2016). Production of recombinant adeno-associated virus vectors using suspension HEK293 cells and continuous harvest of vector from the culture media for GMP FIX and FLT1 clinical vector. *Molecular Therapy*, *24*, 287–297.
49. Blessing, D., Vachey, G., Pythoud, C., Rey, M., Padrun, V., Wurm, F. M., Schneider, B. L., & Deglon, N. (2019). Scalable production of AAV vectors in orbitally shaken HEK293 cells. *Molecular Therapy – Methods & Clinical Development*, *13*, 14–26.
50. Zhao, H., Lee, K. J., Daris, M., Lin, Y., Wolfe, T., Sheng, J., Plewa, C., Wang, S., & Meisen, W. H. (2020). Creation of a high-yield AAV vector production platform in suspension cells using a design-of-experiment approach. *Molecular Therapy – Methods & Clinical Development*, *18*, 312–320.
51. Guan, J.-S., Chen, K., Si, Y., Kim, T., Zhou, Z., Kim, S., Zhou, L., & Liu, X. (2022). Process improvement of adeno-associated virus production. *Frontiers in Chemical Engineering*, *4*, 830421.
52. Rajendra, Y., Balasubramanian, S., & Hacker, D. L. (2017). Large-scale transient transfection of chinese hamster ovary cells in suspension. *Methods in molecular biology* (pp. 45–55). Springer.
53. Bernal, V., Carinhas, N., Yokomizo, A. Y., Carrondo, M. J., & Alves, P. M. (2009). Cell density effect in the baculovirus-insect cells system: A quantitative analysis of energetic metabolism. *Biotechnology and Bioengineering*, *104*, 162–180.
54. Le Ru, A., Jacob, D., Transfiguracion, J., Ansorge, S., Henry, O., & Kamen, A. A. (2010). Scalable production of influenza virus in HEK-293 cells for efficient vaccine manufacturing. *Vaccine*, *28*, 3661–3671.
55. Petiot, E., Cuperlovic-Culf, M., Shen, C. F., & Kamen, A. (2015). Influence of HEK293 metabolism on the production of viral vectors and vaccine. *Vaccine*, *33*, 5974–5981.
56. Côté, J., Garnier, A., Massie, B., & Kamen, A. (1998). Serum-free production of recombinant proteins and adenoviral vectors by 293SF-3F6 cells. *Biotechnology and Bioengineering*, *59*, 567–575.
57. Joshi, P. R. H., Bernier, A., Moço, P. D., Schrag, J., Chahal, P. S., & Kamen, A. (2021). Development of a scalable and robust AEX method for enriched rAAV preparations in genome-containing VCs of serotypes 5, 6, 8, and 9. *Molecular Therapy – Methods & Clinical Development*, *21*, 341–356.
58. Lock, M., Alvira, M. R., Chen, S. J., & Wilson, J. M. (2014). Absolute determination of single-stranded and self-complementary adeno-associated viral vector genome titers by droplet digital PCR. *Human Gene Therapy Methods*, *25*, 115–125.
59. Furuta-Hanawa, B., Yamaguchi, T., & Uchida, E. (2019). Two-dimensional droplet digital PCR as a tool for titration and integrity evaluation of recombinant adeno-associated viral vectors. *Human Gene Therapy Methods*, *30*, 127–136.
60. Joshi, P. R. H., Cervera, L., Ahmed, I., Kondratov, O., Zolotukhin, S., Schrag, J., Chahal, P. S., & Kamen, A. A. (2019). Achieving high-yield production of functional AAV5 gene delivery vectors via fedbatch in an insect cell-one baculovirus system. *Molecular Therapy – Methods & Clinical Development*, *13*, 279–289.
61. Lins-Austin, B., Patel, S., Mietzsch, M., Brooke, D., Bennett, A., Venkatakrishnan, B., Van Vliet, K., Smith, A. N., Long, J. R., McKenna, R., Potter, M., Byrne, B., Boye, S. L., Bothner, B., Heilbronn, R., & Agbandje-Mckenna, M. (2020). Adeno-associated virus (AAV) capsid stability and liposome remodeling during endo/lysosomal pH trafficking. *Viruses*, *12*, 668.
62. Ferreira, T. B., Carrondo, M. J., & Alves, P. M. (2007). Effect of ammonia production on intracellular pH: Consequent effect on adenovirus vector production. *Journal of Biotechnology*, *129*, 433–438.
63. Patel, S. D., Papoutsakis, E. T., Winter, J. N., & Miller, W. M. (2000). The lactate issue revisited: Novel feeding protocols to examine inhibition of cell proliferation and glucose metabolism in hematopoietic cell cultures. *Biotechnology Progress*, *16*, 885–892.
64. Tran, M. Y., & Kamen, A. A. (2022). Production of lentiviral vectors using a HEK-293 producer cell line and advanced perfusion processing. *Frontiers in Bioengineering and Biotechnology*, *10*, 887716.
65. Mendes, J. P., Fernandes, B., Pineda, E., Kudugunti, S., Bransby, M., Gantier, R., Peixoto, C., Alves, P. M., Roldao, A., & Silva, R. J. S. (2022). AAV process intensification by perfusion bioreaction and integrated clarification. *Frontiers in Bioengineering and Biotechnology*, *10*, 1020174.
66. Cervera, L., Gutiérrez-Granados, S., Martínez, M., Blanco, J., Gòdia, F., & Segura, M. M. (2013). Generation of HIV-1 Gag VLPs by transient transfection of HEK 293 suspension cell cultures using an optimized animal-derived component free medium. *Journal of Biotechnology*, *166*, 152–165.
67. Hildinger, M., Baldi, L., Stettler, M., & Wurm, F. M. (2007). High-titer, serum-free production of adeno-associated virus vectors by polyethyleneimine-mediated plasmid transfection in mammalian suspension cells. *Biotechnology Letters*, *29*, 1713–1721.
68. Lavado-García, J., Jorge, I., Cervera, L., Vázquez, J., & Gòdia, F. (2020). Multiplexed quantitative proteomic analysis of HEK293 provides insights into molecular changes associated with the cell density effect, transient transfection, and virus-like particle production. *Journal of Proteome Research*, *19*, 1085–1099.
69. Dash, S., Sharon, D. M., Mullick, A., & Kamen, A. A. (2022). Only a small fraction of cells produce assembled capsids during transfection-based manufacturing of adeno-associated virus vectors. *Biotechnology and Bioengineering*, *119*(6), 1685–1690.
70. Joshi, P. R. H., Venereo-Sanchez, A., Chahal, P. S., & Kamen, A. A. (2021). Advancements in molecular design and bioprocessing of recombinant adeno-associated virus gene delivery vectors using the insect-cell baculovirus expression platform. *Biotechnology Journal*, *16*, 2000021.
71. Elias, C. B., Zeiser, A., Bédard, C., & Kamen, A. A. (2000). Enhanced growth of sf-9 cells to a maximum density of 5.2×107 cells per mL and production of β-galactosidase at high cell density by fed batch culture. *Biotechnology and Bioengineering*, *68*, 381–388.
72. Meghrous, J., Aucoin, M. G., Jacob, D., Chahal, P. S., Arcand, N., & Kamen, A. A. (2005). Production of recombinant adeno-associated viral vectors using a baculovirus/insect cell suspension culture system: From shake flasks to a 20-L bioreactor. *Biotechnology Progress*, *21*, 154–160.
73. Mena, J. A., Aucoin, M. G., Montes, J., Chahal, P. S., & Kamen, A. A. (2010). Improving adeno-associated vector yield in high density insect cell cultures. *The Journal of Gene Medicine*, *12*, 157–167.
74. Bennett, A., Patel, S., Mietzsch, M., Jose, A., Lins-Austin, B., Yu, J. C., Bothner, B., McKenna, R., & Agbandje-Mckenna, M. (2017). Thermal stability as a determinant of AAV serotype identity. *Molecular Therapy – Methods & Clinical Development*, *6*, 171–182.
75. Bereiter-Hahn, J., Munnich, A., & Woiteneck, P. (1998). Dependence of energy metabolism on the density of cells in culture. *Cell Structure and Function*, *23*, 85–93.
76. Jang, M., Pete, E. S., & Bruheim, P. (2022). The impact of serum-free culture on HEK293 cells: From the establishment of suspension and adherent serum-free adaptation cultures to the investigation of growth and metabolic profiles. *Frontiers in Bioengineering and Biotechnology*, *10*, 964397.
77. Martinez, V., Gerdtzen, Z. P., Andrews, B. A., & Asenjo, J. A. (2010). Viral vectors for the treatment of alcoholism: Use of metabolic flux analy-

sis for cell cultivation and vector production. *Metabolic Engineering*, *12*, 129–137.
78. Nadeau, I., Sabatie, J., Koehl, M., Perrier, M., & Kamen, A. (2000). Human 293 cell metabolism in low glutamine-supplied culture: Interpretation of metabolic changes through metabolic flux analysis. *Metabolic Engineering*, *2*, 277–292.
79. Petiot, E., Jacob, D., Lanthier, S., Lohr, V., Ansorge, S., & Kamen, A. A. (2011). Metabolic and kinetic analyses of influenza production in perfusion HEK293 cell culture. *BMC Biotechnology*, *11*, 84.
80. Shen, C. F., Voyer, R., Tom, R., & Kamen, A. (2009). Reassessing culture media and critical metabolites that affect adenovirus production. *Biotechnology Progress*, *26*, NA–NA.
81. Bosma, B., Du Plessis, F., Ehlert, E., Nijmeijer, B., De Haan, M., Petry, H., & Lubelski, J. (2018). Optimization of viral protein ratios for production of rAAV serotype 5 in the baculovirus system. *Gene Therapy*, *25*, 415–424.
82. Grieger, J. C., Snowdy, S., & Samulski, R. J. (2006). Separate basic region motifs within the adeno-associated virus capsid proteins are essential for infectivity and assembly. *Journal of Virology*, *80*, 5199–5210.
83. Girod, A., Wobus, C. E., Zádori, Z., Ried, M., Leike, K., Tijssen, P., Kleinschmidt, J. A., & Hallek, M. (2002). The VP1 capsid protein of adeno-associated virus type 2 is carrying a phospholipase A2 domain required for virus infectivity. *Journal of General Virology*, *83*, 973–978.
84. Sonntag, F., Bleker, S., Leuchs, B., Fischer, R., & Kleinschmidt, J. A. (2006). Adeno-associated virus type 2 capsids with externalized VP1/VP2 trafficking domains are generated prior to passage through the cytoplasm and are maintained until uncoating occurs in the nucleus. *Journal of Virology*, *80*, 11040–11054.
85. Venkatakrishnan, B., Yarbrough, J., Domsic, J., Bennett, A., Bothner, B., Kozyreva, O. G., Samulski, R. J., Muzyczka, N., McKenna, R., & Agbandje-McKenna, M. (2013). Structure and dynamics of adeno-associated virus serotype 1 VP1-unique N-terminal domain and its role in capsid trafficking. *Journal of Virology*, *87*, 4974–4984.
86. Stahnke, S., Lux, K., Uhrig, S., Kreppel, F., Hosel, M., Coutelle, O., Ogris, M., Hallek, M., & Buning, H. (2011). Intrinsic phospholipase A2 activity of adeno-associated virus is involved in endosomal escape of incoming particles. *Virology*, *409*, 77–83.
87. Francois, A., Bouzelha, M., Lecomte, E., Broucque, F., Penaud-Budloo, M., Adjali, O., Moullier, P., Blouin, V., & Ayuso, E. (2018). Accurate titration of infectious AAV particles requires measurement of biologically active vector genomes and suitable controls. *Molecular Therapy – Methods & Clinical Development*, *10*, 223–236.
88. U. S. (2011). Food and Drug Administration, Guidance for Industry: Potency Tests for Cellular and Gene Therapy Products.
89. Gao, K., Li, M., Zhong, L., Su, Q., Li, J., Li, S., He, R., Zhang, Y., Hendricks, G., Wang, J., & Gao, G. (2014). Empty virions in AAV8 vector preparations reduce transduction efficiency and may cause total viral particle dose-limiting side effects. *Molecular Therapy – Methods & Clinical Development*, *1*, 20139.
90. Mingozzi, F., & High, K. A. (2007). Immune responses to AAV in clinical trials. *Current Gene Therapy*, *7*, 316–324.
91. Robert, M.-A., Chahal, P. S., Audy, A., Kamen, A., Gilbert, R., & Gaillet, B. (2017). Manufacturing of recombinant adeno-associated viruses using mammalian expression platforms. *Biotechnology Journal*, *12*, 1600193.

SUPPORTING INFORMATION

Additional supporting information can be found online in the Supporting Information section at the end of this article.

How to cite this article: Moço, P. D., Xu, X., Silva, C. A. T., & Kamen, A. A. (2023). Production of adeno-associated viral vector serotype 6 by triple transfection of suspension HEK293 cells at higher cell densities. *Biotechnology Journal*, *18*, e2300051. https://doi.org/10.1002/biot.202300051